Development and Application of High-Speed Laser Visualization Techniques in Combustion Research

Marcus Aldén and Mattias Richter

Abstract In order to fulfil the requirements of available energy resources, there is a great need to obtain a sustainable and environmentally friendly energy utilization using combustion processes. In order to do this, it is of utmost importance to utilize non-intrusive diagnostic techniques with high spatial and temporal resolution which can characterize the combustion process and also validate combustion models. During the last decades different laser techniques have proven to fulfil these requirements. A special requirement in practical applications when highly turbulent flames are to be investigated, is to be able to follow the phenomena in time, i.e. it is important to develop and apply high speed laser diagnostics. In the present chapter we are describing the use of high speed lasers together with high speed detectors which make it possible to probe in two dimensions even the fastest combustion phenomena in real time. The chapter is describing the use of a so called Multi YAG laser which together with a framing camera is able to record up to eight images. Also the use of a high repetition rate laser and a high power burst laser together with CMOS cameras and their application for studies of turbulent combustion phenomena are described. The examples are mainly taken from the author's laboratory and include more academic studies of turbulent flames but also practical applications in engines.

M. Aldén (✉) · M. Richter
Division of Combustion Physics, Lund University, Lund, Sweden
e-mail: marcus.alden@forbrf.lth.se

M. Richter
e-mail: mattias.richter@forbrf.lth.se

1 Introduction

Thermochemical conversion processes, mainly combustion, constitute very important phenomena in our society. A quantitative description of flames and combustion phenomena is still lacking due to the extreme complexity of these thermal-mechanical-chemical phenomena involving hundreds or even thousands of elementary chemical reactions, turbulent flows, heat transfer and multi-phase interactions. Scientifically, combustion thus involves a wide range of basic and applied disciplines. The continued development of these processes requires inter-disciplinary scientific research and professional personnel with wide and detailed knowledge in various fields. Specifically, the main reasons for doing scientific research on combustion and related processes are:

- Combustion processes provide a major source of energy for our society ($\sim$>90%).
- Emissions from combustion processes constitute a major part of the air pollutants of today, >90% of NO_x and >50% of SO_x originate from combustion devices. Soot, polycyclic aromatic hydrocarbons and particulates are other major air pollutants emerging from combustion. Another environmental aspect of combustion of fossil fuels is the substantial emission of greenhouse gases, e.g. carbon dioxide, which put emphasis on combustion of new, e.g. bio-based renewable fuels.
- Knowledge in combustion science and technology is crucial for main branches of industry, e.g. the transportation industry, the heat and power industry and the manufacturing industry.
- Combustion processes have important effects on our society, for example in the areas of domestic heating, waste incineration, and prevention and extinguishing of unwanted fires.

With the outstanding scientific/technical challenges in combustion science there is a great need for development of new instrumentation tools as well as appropriate models to face and approach several research barriers e.g.:

- Turbulent combustion, with extreme temporal and spatial scales requiring adequate measurement and modeling resolution
- Combustion of renewable fuels with unknown composition and thus requiring adequate chemical modeling and new diagnostics
- Control, understanding and avoidance of combustion instabilities/oscillations, requiring for example ultra-high temporal resolution, both in modeling and experiments
- High pressure combustion; the chemistry become much more challenging when going from atmospheric pressure to tens or hundreds of bars, i.e. pressures relevant for industrial conditions
- Understanding of multi-phase conversion phenomena

In order to optimize and control combustion processes, it is of utmost importance to apply diagnostic techniques capable of measuring critical parameters. The

challenges in this environment can be substantial; high temperature, high pressure, high contents of particles/droplets and a highly turbulent flow field. During the last decades the most important development for a deepened understanding of combustion processes in terms of experimental achievements, has been the introduction of various laser diagnostic techniques. The advantages with these techniques are their inherent non-intrusiveness in combination with high temporal and spatial resolution. Various techniques have been developed for measurements of species concentrations, temperatures and velocities, see e.g. [1–5] yielding possibilities for instantaneous information in two, three or even four dimensions (space + time).

Until the late nineties more or less all combustion studies yielding two-dimensional information, were made using lasers with a repetition rate of ∼10–100 Hz. For this purpose different techniques, e.g. Mie scattering, planar laser-induced fluorescence (PLIF), Laser-induced incandescence (LII), were applied for measurements of particle/droplets, atoms and molecules and soot characteristics, respectively. Clearly, at these frequencies there are no way to follow the turbulent structures at the length scales prevailing in most applied combustion environments, e.g. turbulent combustion taking place in engines and gas turbines. More or less the only commercially available high speed laser at that time used for combustion diagnostics was the copper vapor laser. These lasers typically run at a repetition rates over 10 kHz and produces radiation at 511 and 578 nm. However, the practical applications have been scares due to a rather low pulse energy, ∼ couple of mJ, and a low efficiency when pumping dye lasers. Thus, the applicability in combustion has been limited to Mie scattering and particle image velocimetry (PIV) in practical combustion applications such as Internal Combustion (IC) engines [6, 7].

In the present chapter we will review the development and application of high speed visualization using advanced lasers/detectors for studies of combustion phenomena. Most of the examples will be given from the activities at Lund University. The first section will describe a specially designed laser/detector system for high speed visualization using a limited number of high energy pulses. In the next section application of a continuously operating pulsed high speed laser, ∼ 10 kHz, will be described. This equipment complements the specially designed laser in the sense that it provides an endless pulse train, but it also suffers from significantly lower pulse energies. Finally, a newly available commercial laser, based on a burst system with 100–1000 pulses and still high pulse energies, will be described.

2 A Tailor Made Laser/Detector System for High Speed Visualization: A Multi-YAG Laser and Framing Cameramen Description

### 2.1 Instrument Description

As described above, there has been a strong need for a versatile and useful laser/detector system for studies of turbulent combustion phenomena. In order to
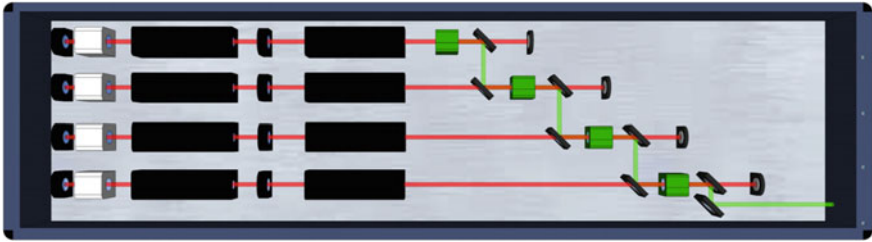
Fig. 1 Schematic overview of the Nd:YAG laser cluster, consisting of 4 Nd:YAG lasers

make high speed visualization of combustion processes a specially designed laser/detector system was developed in Lund in the late nineties. The system consists of a Nd:YAG laser cluster and a high speed camera. It is capable of producing a rapid sequence of up to 8 laser pulses with a temporal separation ranging from microseconds to milliseconds. The laser source of the high speed laser diagnostic system is a cluster consisting of 4 flash lamp pumped Nd:YAG lasers. Each laser in the cluster consists of a Q-switched Nd:YAG oscillator and a single amplifier, emitting laser pulses with a duration of 7 ns. After each oscillator there is a manual attenuator, consisting of two polarizers with a rotatable half-wave plate in between, which allows continuous adjustment of the laser pulse energy without changing the thermal load on the Nd:YAG crystals. The beams from the four lasers are combined using a scheme illustrated in Fig. 1. The laser beam from the first laser is converted from 1064 to 532 nm, using a second harmonic generation crystal. This beam is then combined with the 1064 nm beam from the second laser using a dichroic mirror, reflecting 532 nm and transmitting 1064 nm. The combined beams then pass through the second harmonic generation crystal of the second laser, the 532 nm beam passes unaffected while the 1064 nm beam is converted to 532 nm. The same procedure is then repeated two more times until all four beams have been combined. The large number of optical components in the beam path of lasers 1 and 2 introduces some energy losses and beam profile degradation. The energy losses can, however, be compensated for by increasing the flash lamp pump intensity of these lasers. It is also possible to use an alternative beam combining scheme, where beams having different polarization orientations are combined. The advantage of the latter scheme is that fewer optical components are needed, minimizing energy losses and beam profile degradation. On the other hand beam alignment is more critical and difficult to achieve.

A single fourth harmonic generation crystal, converting the 532 nm pulse train to 266 nm can optionally be inserted near the output of the unit. The four individual lasers can be fired in series with time delays, τ_1, ranging from 0 up to 100 ms, where the upper limit is given by the overall repetition frequency of the system (10 Hz). By switching the Q-switch twice during the flash-lamp discharge duration, each of the Nd:YAG lasers can be fired two times with a short separation, τ_2, between pulses. τ_2 can be adjusted from 25 to 145 µs, limited by the length of the flash lamp discharge and the gain build up time in the oscillator. The pulse timing is
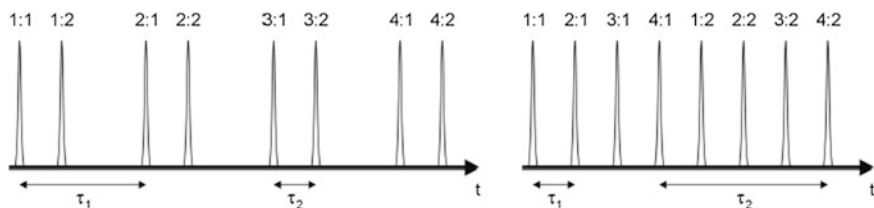
Fig. 2 Timing diagram for a pulse burst from the Nd:YAG laser cluster, *left* the double pulses from each laser are fired in series, *right* the double pulses are interleaved

Table 1 Nd:YAG laser cluster output energies

|	Multi YAG energy output in each pulse (mJ)
	Single/double pulse operation
Laser energy at 532 nm	880/325
Laser energy at 355 nm	360/220
Laser energy at 266 nm	180/70

illustrated in Fig. 2. By interleaving the double pulses from the four lasers the time separation between pulses can be reduced down to 6.25 µs (=25 µs/4), as shown to the right in Fig. 2. It should be noted that the laser pulses do not have to be equally spaced as shown, as the timing of each laser is individually controllable.

The multi-YAG laser system can also generate 355 nm radiation. As 355 nm generation requires mixing 532 and 1064 nm this cannot be done using a single third-harmonic-generating (THG) crystal in a manner similar to 266 nm generation. Instead, each laser beam is individually doubled to 532 nm and tripled to 355 nm using a THG crystal. The 355 nm beam is separated from the 1064 and 532 nm beams using a dielectric mirror (coated high reflective—355 nm, high transmission —532 nm and high transmission—1064 nm). The beams at 355/532 nm from the individual lasers are then combined in a scheme similar to the 532/1064 nm combining illustrated in Fig. 1.

Maximum pulse energies of the Multi-YAG laser system are given in Table 1.

To be able to excite specific species using for example laser-induced fluorescence, it is required to convert the primary laser beams from the YAG cluster to tunable radiation. This can be made using a single dye laser, providing the dye solution is flowing in a sufficient speed to replace the liquid solution between two consecutive laser pulses [8] or to pump several dye lasers [9]. A third alternative is to use an optical parametric oscillator, OPO. Very simplistically, an OPO splits one photon into two with lower frequency. As the energy in the each of the two photons is dependent on the angle of the active crystal, the output wavelength can be scanned by turning the crystal [10].

When using the multi-YAG laser system it is clearly very important to use a high-speed camera which can match the repetition rate of the laser system. The requirement of the camera speed is thus in the MHz regime. Furthermore, in order
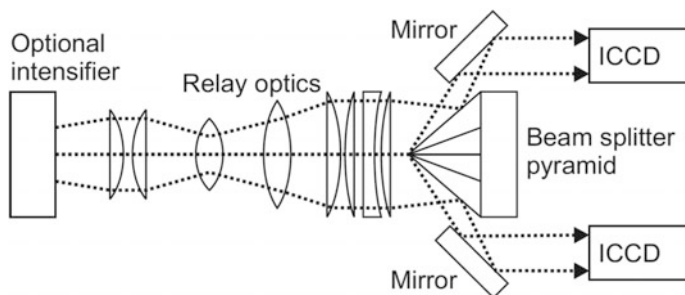
Fig. 3 A sketch of a Framing camera used in the high-speed measurements together with the Multi-YAG cluster. (Only two of the eight ICCDs around the pyramid beam splitter are shown)

to be able to measure low level signals, the efficiency of the camera is a very important parameter. In the experiments in Lund two framing cameras (Imacon 468 and SIM 8) have been used. The cameras have a similar general structure but they have a slightly different construction. Both cameras use eight individual ICCD's (intensified CCD) that can be triggered individually. This allows for frame rates up to 100 MHz but limits the number of frames to eight per event. When using the Framing cameras a single optical input lens is used so that all eight ICCDs see and image the same measurement object. In order to both amplify the signal and to convert the incoming light to be optimum for the optics and intensifiers in the camera, an optional intensifier can be placed after the initial lens. For the SIM 8 (Specialised Imaging, Tring, United Kingdom) camera, two intensifiers with varying phosphor decay time can be used: one with P46 phosphor (300 ns decay time) and one with FS phosphor (12 μs decay time). These decay times determine the minimum time separation between exposures if ghosting is to be avoided. A sketch of a framing camera Imacon 468 (Hadland Photonics, Hertfordshire, United Kingdom) is shown in Fig. 3.

2.2 Examples from Multi-YAG Systems

The first demonstration using the system described above was in experiments performed in a non-premixed methane/air flame consisting of two concentric tubes [11]. Air was passed through the inner tube and fuel was passed through the outer tube. The hydroxyl radical, OH, was excited using the $Q_1(8)$ transition near 282 nm in the $v'' = 0$, $v' = 1$ band of the $X^2\prod^+ \rightarrow A\ ^2\sum$ system. Subsequent fluorescence in the (1, 1) and (0, 0) bands near 309 nm was observed using appropriate optical filters. The laser beams were formed into a sheet 5 cm in height and about 80 μm in width in the interaction region. The laser beam profiles were monitored on line by simultaneously imaging fluorescence from a water solution containing fluorescing dye. Each image was normalized by this profile.
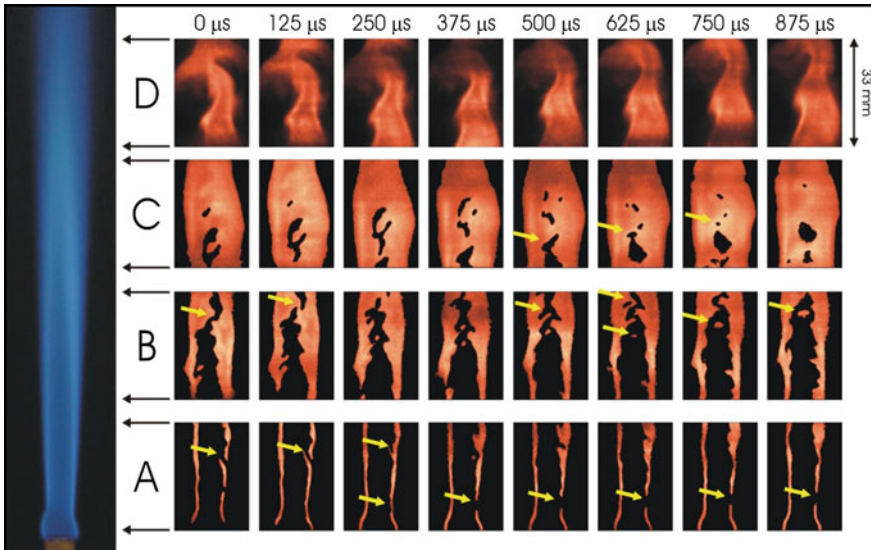
Fig. 4 Temporal PLIF sequences of OH at different heights in the turbulent, non-premixed CH₄/ air-flame: A direct emission photograph of the flame is included to the *left*. Each PLIF-image shown corresponds to a single laser shot, time increases from *left to right* in 125 µs steps. The four measurement regions *A*, *B*, *C*, *D* correspond to the indicated positions in the flame [11], with permission of the Springer

Figure 4 shows typical results obtained from the flame. In the left part a direct emission photograph of the flame is included to identify the regions imaged by the OH-PLIF displayed to the right. Each temporal OH sequence (labelled A to D in the figure) corresponds to an imaged height of 33 mm or about 7 inner nozzle diameters. The time separation between successive images was 125 µs translating into an overall repetition rate of 8 kHz. In region A of Fig. 4, close to the exit nozzle where flow is still laminar, the typical 'braids' of OH can be observed marking regions where fuel and oxidizer diffuse to, and mix in, the reaction zone. Local flame extinction is clearly seen in this sequence (highlighted by arrows). Most likely this is caused by convection building up strong local gradients which effect losses by molecular transport. This leads to a slowing down of chemical reactions to the point where the flame extinguishes. The sequence clearly highlights the capabilities of the technique.

Local extinction phenomena have a major influence on flame stability and a better understanding of the mechanisms leading to extinction is both of fundamental and practical importance. To study the importance of large scale structures for local flame extinction two-dimensional measurements of relevant quantities with high time resolution are desirable. Simultaneous measurements of both flow and flame quantities, allowing correlations between the two to be studied, are also useful in this respect. Simultaneous time resolved measurements of the evolution of the OH radical distribution and the instantaneous velocity field in turbulent flames were presented in Ref. [12]. The combined measurement technique thus allowed the
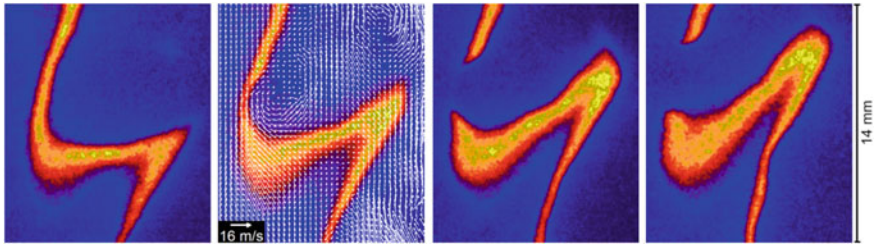
Fig. 5 A local extinction phenomenon around 150 mm above the burner. The time separation between the images is 125 μs. In the second image the velocity field from the PIV measurement is shown in the same figure as the OH-PLIF image [12]

possibility to study the dynamics of turbulence/chemistry interactions. High speed PLIF of OH at repetition rates exceeding 13 kHz was used to track the response of the flame front to the turbulent flow field. From the OH-PLIF sequences the position, in both space and time, where the local extinction of the flame front begins, could be identified. The temporal changes in local OH distribution during the extinction process could also be studied and the time scale of extinction events estimated. Instantaneous velocity field measurements were performed simultaneously using PIV. In the velocity field the flow structures associated with the identified extinction events were visualized. A result from these experiments is shown in Fig. 5. In the first image a flame front is captured. The imaged region corresponds to 14×16 mm and the bottom part is positioned 144 mm over the burner nozzle.

In the second image a vortex is seen, approaching the flame front and forcing it to bulge out slightly, a decrease in the OH concentration can also be seen at the top of the bulge. In the next frame the flame has just extinguished as indicated by the sharpness of the two tips of the now separated flame fronts. The large-scale wrinkling of the flame front in this downstream part of the flame is clearly seen. Three relatively large regions with high and uniformly directed velocities act to twist the already s-shaped flame front even further.

Clearly, the possibility to achieve detailed time resolved information of turbulent combustion phenomena is of instrumental importance for a deepened understanding of these phenomena. In a joint collaboration with University of Stuttgart and NEC Europe, the growth of spark ignited flame kernels in turbulent premixed gases was studied [13]. The growth of the flame kernel starts with an initially laminar kernel moving in the turbulent flow field, it subsequently grows with increasing degrees of wrinkling; and finally develops into a fully turbulent flame. A cylindrical constant-volume combustion cell, equipped with four high speed rotors, was used to study the turbulent flame kernel propagation. The cell was filled with CH_4/air or H_2/air mixtures, which were ignited by a spark in the center of the cell. The ignition system was designed to ensure highly reproducible ignition events. Controlled and variable amounts of turbulence could be generated in the mixture by the four rotors. The flow field in the center was investigated using a Laser Doppler Velocimetry system and the turbulence field was found to be homogeneous and isotropic.
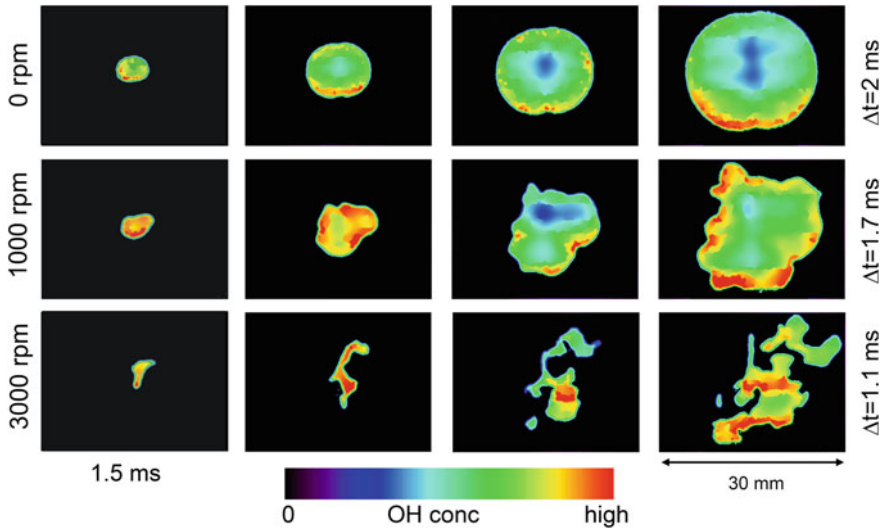
Fig. 6 *Top* OH laminar flame propagation in a stoichiometric CH_4/air mixture with the time separation between images are 2 ms. *Middle* OH-PLIF sequence of turbulent flame propagation (rotor speed = 1000 rpm) in a stoichiometric CH_4/air mixture with a time separation of 1.7 ms. *Bottom* OH-PLIF sequence of turbulent flame propagation (rotor speed = 3000 rpm) in a stoichiometric CH_4/air mixture. Time separation between images is 1.1 ms [13], with the permission of Elsevier

OH-PLIF sequences, consisting of 4 images separated by 250 µs to 2 ms, were recorded, which show a cut through the flame kernel. Parameters like fuel, stoichiometry and turbulence intensity were varied, and a large data set was recorded. In Fig. 6, the interaction between turbulence and chemical reactions is seen in action, as the flame is wrinkled by turbulent eddies. This leads to an increased reaction surface area which increases the overall reaction rate, as indicated by the shorter time between images compared to the laminar flame in the top row. When the rotor speed was increased further (3000 rpm) the flame propagation speed increases as well as the flame front wrinkling, and isolated structures appear in the PLIF images, see Fig. 6, bottom row.

In addition to the more fundamental issues of turbulent combustion phenomena, high speed laser visualization techniques add considerable sharp tools for studying applied combustion process, e.g. taking place in an internal combustion engines. The fuel/air mixing and combustion processes within the cylinder of an IC engine do to a large extent determine the engine efficiency and emissions. Simulations of the two processes can be performed using computational fluid dynamics (CFD), but the current precision of this tool makes in-cylinder diagnostics necessary in order to fully understand fuel/air mixing and combustion. By using the laser/detector system described above cycle-resolved engine measurements can be studied, where single combustion events can be followed in time. Cycle-to-cycle variations of complex events can thus be studied, which is impossible from single shot images captured in

Fig. 7 Schematic setup for performing PLIF imaging in an optical engine. The high-speed Imacon 468 camera is arranged to detect fluorescence from the combustion chamber through the optical piston
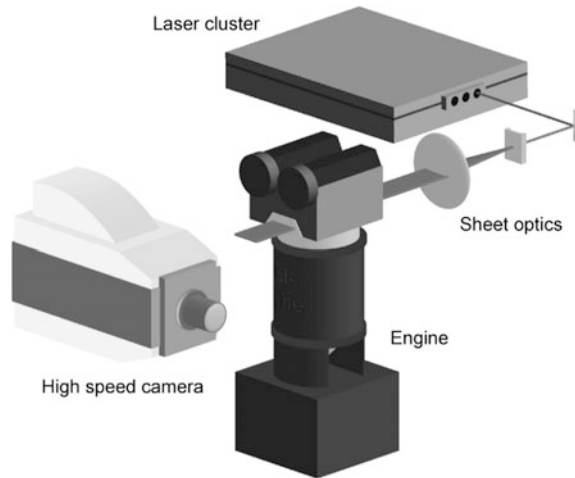
different cycles. As individual structures can be followed in time, the large-scale development of a fuel injection, an ignition event, or a flame propagation can be visualized. Time scales of such phenomena can be estimated from the time resolved data.

In Fig. 7, a typical set-up for high speed visualization in an engine with optical access is shown. Isooctane was used as fuel, and 10% of 3-pentanone was added as fluorescent tracer [8]. In experiments in a spark ignited engine, the early flame propagation was captured by rapidly sequenced fuel tracer PLIF. An example of fuel tracer PLIF is shown in Fig. 8 (top) where eight consecutive images recorded in the same combustion cycle are presented [8]. The combustion chamber is viewed from above with the spark plug located to the upper-right, see photo to the left in Fig. 8 (top). The intensity in the PLIF images is proportional to fuel concentration, which means that bright regions correspond to unburned gases and dark regions to burnt gases. The turbulent flame propagation is illustrated by the expansion of the burnt regions through the sequence. The time separation between consecutive images is 100 μs, which here corresponds to 0.7 crank angle degree (CAD). The first image is acquired at 5 CAD after top dead center (ATDC). The appearance of isolated flame islands in the sequence is an effect of three-dimensional flame wrinkling, in and out of the two-dimensional laser sheet.

In order to compare different engine concepts also a homogenous-compression charge-ignition (HCCI) engine was investigated [8]. In an HCCI engine the pre-mixed fuel/air mixture auto-ignites by compression. In Fig. 8 (bottom) a sequence covering the major part of a combustion event in the HCCI engine is shown, covering 6.5 CAD. The fuel distribution is viewed from below through the trans-parent piston. In the first image (1 CAD ATDC) a homogeneous fuel distribution is seen. In the next image several small dark regions can be found to the left, to the right and in the upper part of the image, indicating that the reactions consuming fuel have started. These chemical reactions are initiated by the temperature rise
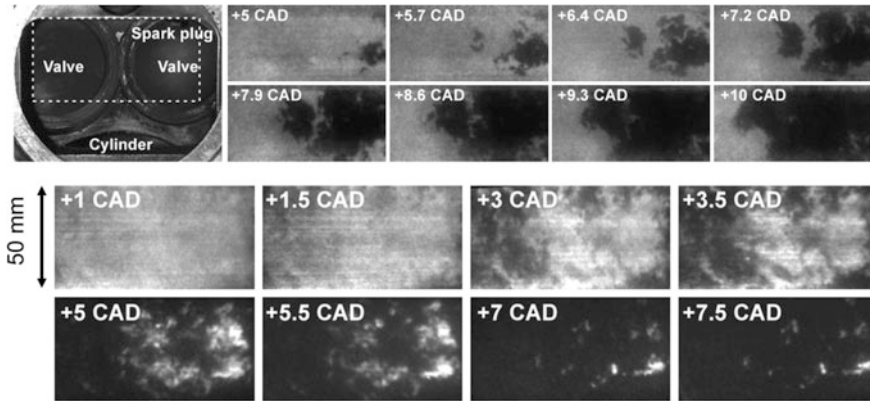
Fig. 8 *Top* Cycle resolved fuel tracer PLIF sequence recorded in a spark ignited (SI) engine. The time separation between consecutive images corresponds to 100 µs (0.72 CAD). The imaged region was 50 × 25 mm², and is shown to the *left*. *Bottom* Fuel tracer PLIF sequence recorded in an HCCI engine. The fuel distribution in a plane in the center of the combustion chamber was imaged through the piston, the imaged region corresponds to 95 × 50 mm² [8], with permission of the Optical Society

associated with the compression of the gas. The fuel in these regions is then consumed further in the next images, the regions spread and new regions of fuel consumption also appear. The HCCI combustion is rapid, in 3.5 crank angle degrees most of the fuel is consumed, and, in the end (7.5 CAD ATDC) only small separated islands of fuel remain. The use of unequal time spacing between images throughout the series allows a long event to be captured, while short term changes are still captured between image pairs.

3 Continuous KHz Repetition Rate Laser Applications

During the last decade, Diode Pumped Solid State (DPSS) lasers have gradually become more powerful and can nowadays be a viable alternative in high repetition rate two-dimensional (2D) imaging in reacting flows. Instead of employing flash lamps as pump source, as found in most 10-Hz systems and laser clusters such as the one described earlier, the gain medium is here pumped by radiation from a diode array. Compared to gas discharge lamps, the spectral profile of the emission is more narrow for the diodes. This results in a more efficient pumping, with less waste heat generated. The main advantage with the DPSS laser systems is their ability to operate continuously at relatively high ($\sim$20 kHz) repetition rates. This feature brings several distinct benefits to the field of combustion diagnostics. One is the ability to follow a relatively slow transition with overlaid rapid changes. Another advantage is the possibility to utilize the post-triggering capability of

modern CMOS detectors. This can be used to capture rare events such as flame extinction or re-ignition processes where accurate pre-triggering is very hard.

The main drawback with the commercially available DPSS-systems is the limited pulse energy compared to the conventional 10 Hz systems or the Multi-YAG cluster mentioned earlier. Typically, the pulse energy is two orders of magnitude lower for the DPSS. See Refs. [14–18] for different applications of high speed lasers/detectors for combustion applications.

One further example of an application where the continuous high repetition rate output is utilized is in temporally resolved three-dimensions imaging, i.e. 4D imaging, of fluids [19]. The technique is based on rapid scanning of a thin laser sheet across the volume of interest. Each exposure of the signal generated within the laser sheet represents a 2D distribution of the species of interest. Between the individual exposures, the laser sheet is translated perpendicular to the plane. Hence, the spatial position of the probe volume is slightly altered. Through interpolation the 2D data in different cross sections can be combined to show 3D information. It is important to perform each sweep across the investigated volume fast enough to freeze the fluid motion. If there is a small but still significant motion of the fluid during the scan there are measures that can be applied to compensate for this in post-processing. More details on the practical implementation can be found in [19]. In Fig. 9, a schematic setup for performing 4D imaging of OH radicals in a Bunsen flame is shown. The DPSS YAG-laser (Edgewave HD40IV-E, Edgewave GmbH, Würselen, Germany) is operated close to its maximum repletion rate of 20 kHz. A high repetition rate dye laser (Sirah Credo, Sirah Lasertechnik GmbH, Grevenbroich, Germany) is used to convert the 532 nm radiation from the YAG to 609 nm. After frequency doubling and fine tuning of the wavelength output,
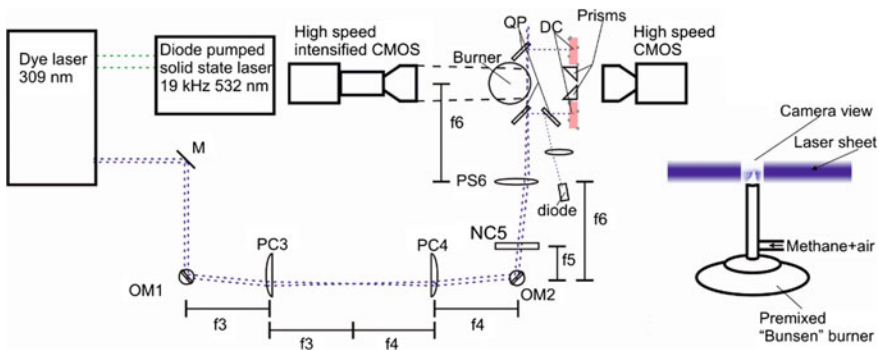
Fig. 9 Schematic setup for acquisition of 4D data through application of the rapid scanning technique. Note the use of dual oscillating mirrors to make the sheet separation more equidistant than what can be achieved with a single oscillating mirror. *M* Mirror, *f* focal length, *DC* Dye Quvette, *QP* Quartz plate, *OM* Oscillating mirror, *PC* Pos. Cyl. Lens, *NC* Neg. Cyl. lens, *PS* Pos. Spherical lens reprinted from R. Wellander, Exp. Fluids 55 (2014), with permission of Springer
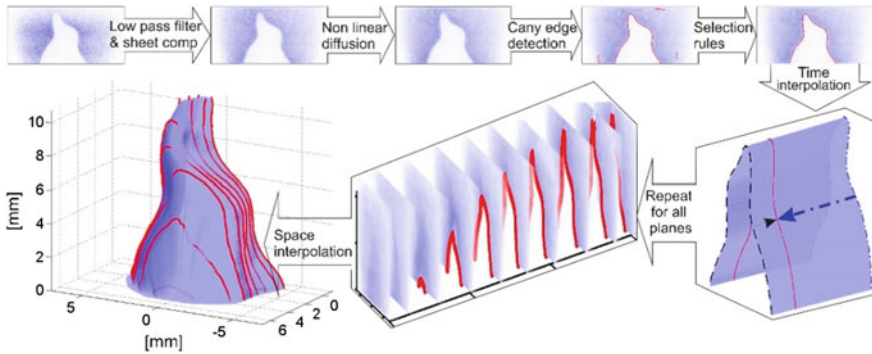
Fig. 10 Illustration of the image processing steps employed when creating 3D images from the 2D images recorded in a rapid sequence in different spatial positions across the probed volume reprinted from R. Wellander, Exp. Fluids 55 (2014), with permission of Springer

309 nm radiation matching a transition in the OH radical, is generated. The translation of the laser sheet in between exposures is achieved through implementation of two oscillating mirrors. In principle the deflection of the beam could be realized with one oscillating mirror. The sheet displacement would then be oscillating around the center point in a sinusoidal manner. However, by using two mirrors positioned according to the sketch and forcing the second mirror to oscillate at three times the frequency of the first mirror, the displacement will approach a triangular pattern. For more details on the mirror system please refer to [19, 20].

In conventional 2D PLIF imaging as described earlier, often the weak fluorescence signals are maximized through use of low f-number optics. The resulting restriction in the depth of field is then not an issue since the imaged volume, that is defined by the laser sheet, is generally very thin. However, in 4D imaging performed with a scanning light sheet the required depth of field is governed by the extension of the scanned volume. In order to achieve a sufficient depth of field the f-number must here most often be increased. This is obviously a limiting factor and the resulting tradeoff between signal-to-noise ratio and depth of field must be considered when probing species with weak fluorescence signals.

The image processing steps applied to the originally recorded 2D images and the following interpolation to achieve the 3D images are illustrated in Fig. 10. With this set-up it is possible to generate 3D images, reconstructed from ten 2D images, at a repetition rate of 2 kHz. In Fig. 11, a series of OH iso-concentration surfaces, recorded with a Photron SA-Z, are illustrated.
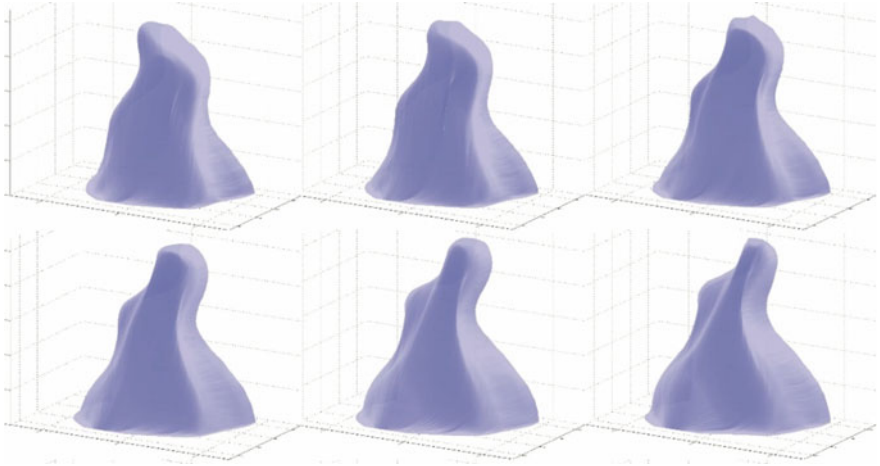
Fig. 11 Example of temporally resolved 3D iso-concentration surfaces of OH radicals in a laboratory flame. The 3D images are recorded at a repetition rate of 2 kHz reprinted from R. Wellander, Exp. Fluids 55 (2014), with permission of Springer. The corresponding movie is available online
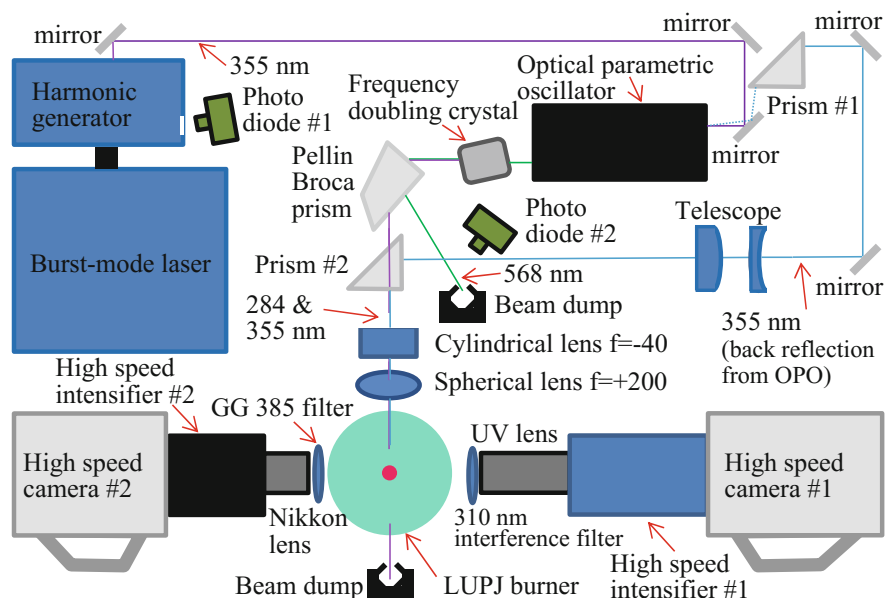
4   High Power Burst Laser Application

Burst-mode lasers for combustion diagnostics were introduced in the late 1990s [21, 22]. These systems are based on sequential amplification of a high repetition rate seed laser. Until recently, burst mode lasers were quite rare and not commercially available. Fortunately, this has now changed and in this section results from the application of a state-of-the-art ultra-high speed burst-laser (QuasiModo, Spectral Energies LLC, Dayton, Ohio, USA) will be shown. This laser is a hybrid-pumped burst-mode laser with two diode-pumped amplifiers followed by six flash-lamp pumped amplifiers. Two 6 mm flash-lamp pumped amplifiers serve as a double-pass for the laser beam in order to increase the gain. The beam is then further amplified by passing through four additional flash-lamp pumped amplifiers, see Fig. 12.

The duration of each burst is adjustable up to 10 ms. Also the repetition rate is adjustable from 10 to several hundred kHz. There is, of course, a tradeoff between pulse energies and rep rate. As an example, if the laser is operated at 10 kHz with a burst duration of 10 ms, the resulting pulse train will consist of 100 pulses. In terms of individual pulse energies, peak values for the available wavelengths will be approximately >1200 mJ at 1064 nm, >600 mJ at 532, >300 at 355 nm, >70 mJ at 266 nm. These numbers are typically about 50 times higher than the corresponding pulse energies from a continuously operating DPSS YAG. On the detector side these systems rely on conventional CMOS technology.

Figure 13 illustrates the experimental setup for simultaneous dual-species visualization of a premixed turbulent jet flame by using ultra-high speed PLIF imaging (50–100 kHz). The burner is a hybrid porous-plug/jet type burner,

Fig. 12 Layout of the Quasimodo Burst-laser. The output from a cw fiber laser is shopped by an acoustic-optical modulator. The resulting high-rep rate pulse train is then sequentially amplified in the YAG-rods (labeled 2.8, 4, 9.5, 12.7 mm)

described in more detail in [23]. Its main parts are a porous sintered stainless steel plug with a diameter of 61 mm and a 1.5 mm-diameter nozzle in the center for the creation of a jet flame. Premixed CH_4 and air mixture was fed through the center nozzle to create the jet flame which was stabilized by a premixed CH_4-air flame above the porous plug referred to as co-flow. In the examples presented here the jet velocity was set to 66 m/s.

The OPO was pumped by 355 nm radiation from the burst system and produced excitation radiation for OH near 284 nm. The excitation of formaldehyde (CH_2O) can conveniently be performed at 355 nm. Thus, the residual 355 nm remaining after pumping the OPO was used for this purpose. The two beams were then formed into thin sheets and overlapped in the center of the jet-flame. The gate time, i.e. exposure time, of both high-speed intensifiers was set to 100 ns. At 100 ns exposure time, all the generated fluorescence signals were captured while the background signals caused by the flame chemiluminescence were sufficiently suppressed.

Experimental results generated with this setup are presented in Figs. 14 and 15. The burst system is capable of providing excitation energies comparable or even exceeding the ones from Multi-YAG lasers but for a significantly longer pulse train. This facilitates the following of interesting phenomena such as variations in

Fig. 13 Experimental setup for simultaneous PLIF imaging of OH and CH$_2$O at 50 kHz in a turbulent jet-flame. Two high-speed cameras in combination with two high-speed intensifiers are mounted opposite to each other in order to capture OH and CH$_2$O fluorescence simultaneously. For detecting the former species, a CMOS Photron Fastcam SA-Z (camera #1) was used in combination with a high-speed intensified relay optics. For the CH$_2$O imaging, a CMOS Photron Fastcam SA-X2 (camera #2) was employed which was also combined with a high-speed image intensifier (Lambert HS) (Courtesy of Zhenkan Wang)
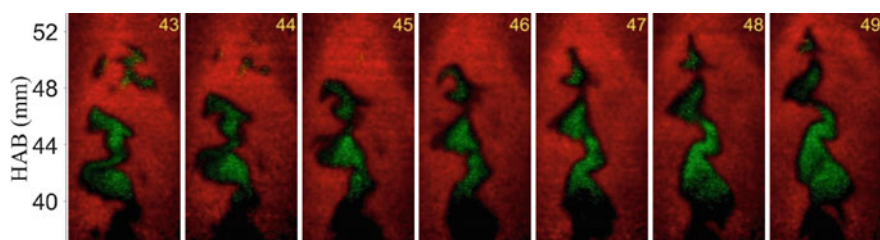
Fig. 14 Simultaneous PLIF recordings of OH (*red*) and CH$_2$O (*green*) performed at 50 kHz in a turbulent flame (Courtesy of Zhenkan Wang)

turbulent length scales, extinction and re-ignition over longer periods of time. In Fig. 14, the repetition rate was set to 50 kHz. To further demonstrate the capability of this unique system the repetition rate was increased to 100 kHz for the formaldehyde distribution sequence presented in Fig. 15. As indicated by the still sufficient signal-to-noise ratio, the frame rate could be increased further. The laser and detector allow for up 500 kHz with reduced pixel number.

Fig. 15 Formaldehyde distributions in a turbulent jet-flame recorded at different heights above the burner for different air-fuel ratios. The burst laser excitation source and the intensified CMOS camera were operated at 100 kHz (Courtesy of Zhenkan Wang)
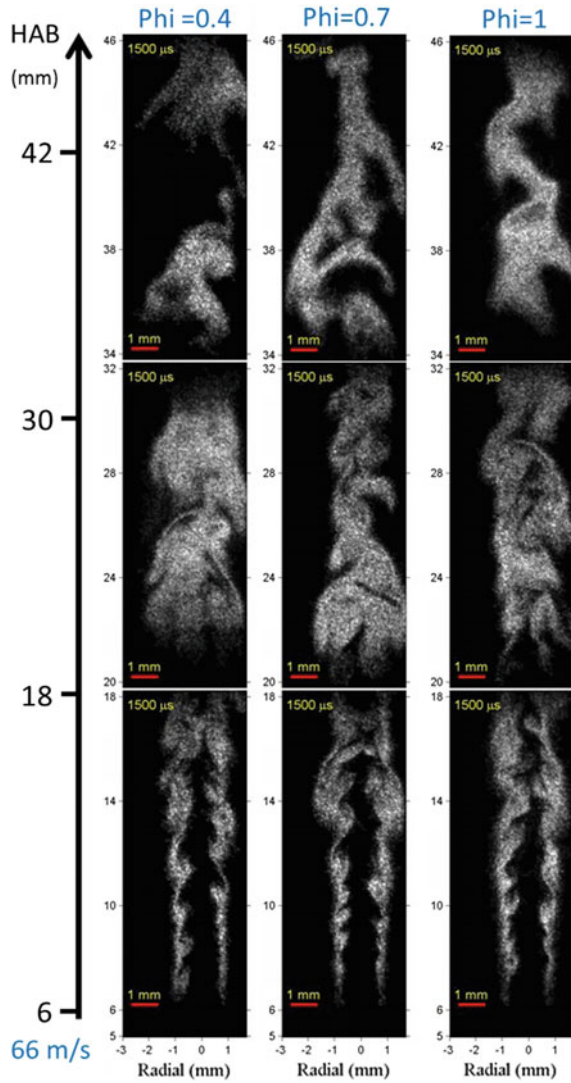
Another possibility with the burst system is to perform PIV measurements at extreme speeds. Since the pulse train is originally generated from a continuous wave laser, the pulse separation can be adjusted arbitrary. For high repetition rate PIV measurements the pulses can be arranged in pairs with short separation between the two pulses in each pair and longer separation between the pairs. The energies available indicate that PIV at 100 kHz should be fully feasible.

5   Summary and Conclusion

As have been demonstrated in this Chapter the use of high speed laser imaging for visualization of combustion parameters is of utmost importance in gaining new information about the physics and chemistry controlling phenomena related to turbulent combustion. Moreover, since industrial applications more or less always rely on turbulence, the benefits that can be achieved using these new diagnostic tools are multifold. Clearly, the interaction with expertise in computational fluid dynamics is also crucial to address the most important phenomena for model validation.

It can thus be foreseen that the use of high speed visualization of combustion phenomena, both in the laboratory and in various industrial applications, will be a major tool for future combustion applications.

A disadvantage with the high-speed measurements as described above is the high cost for both lasers and detectors. A very new and promising technique for some high speed/3D applications is to use the Frequency Recognition Algorithm for Multiple Exposure technique [24]. Using this approach simultaneous imaging of several images with one detector and several structured laser sheets, originating from one laser, can be achieved [24]. The different images are then separated in the Fourier space providing either high speed imaging with a framing speed only limited by the laser pulse length or instantaneous 3D imaging.

References

1. A.C. Eckbreth, *Laser Diagnostics for Combustion Temperature and Species* (Gordon and Breach Publisher, 1996)
2. K. Kohse-Höinghaus, J.B. Jeffries (eds.), *Applied Combustion Diagnostics* (Taylor and Francis, New York, 2002)
3. K. Kohse-Höinghaus, R.S. Barlow, M. Aldén, J. Wolfrum, Combustion at the focus: laser diagnostics and control. P. Combust. Inst. **30**, 89–123 (2005)
4. M. Aldén, J. Bood, Z. Li, M. Richter, Visualization and understanding of combustion processes using spatially and temporally resolved laser diagnostic techniques. P. Combust. Inst. **33**, 69–97 (2011)
5. M. Aldén, A. Omrane, M. Richter, G. Särner, Thermographic phosphors for thermometry: a survey of combustion applications. Prog. Energ. Combust. **37**, 422–461 (2011)
6. I. Duwel, M.C. Drake, T.D. Fansler, High-speed, high-resolution imaging of multihole fuel sprays in a firing spray-guided direct-injection gasoline engine. Paper presented at ILASS-Europe 19th annual conference, Nottingham, England, 2004
7. M. Reeves, D.P. Towers, B. Tavender, C.H. Buckberry, A high-speed all digital technique for cycle-resolved 2-D flow measurement and flow visualization within SI engine cylinders. Opt. Laser. Eng. **31**, 247–261 (1999)

8. J. Hult, M. Richter, J. Nygren, M. Alden, A. Hultqvist, M. Christensen, B. Johansson, Application of a high-repetition-rate laser diagnostic system for single-cycle-resolved imaging in internal combustion engines. Appl. Optics **41**, 5002–5014 (2002)

9. J. Olofsson, *Laser Diagnostic Techniques with Ultra-High Repetition Rate for Studies in Combustion Environments* (Lund University, Dissertaton, 2007)

10. J. Sjöholm, E. Kristensson, M. Richter, M. Alden, G. Goritz, K. Knebel, Ultra high speed pumping of an OPO laser, for high speed laser-induced fluorescence measurements. Meas. Sci. Technol. **20**, 025306 (2009)

11. C.F. Kaminski, J. Hult, M. Aldén, High repetition rate planar laser induced fluorescence of OH in a turbulent non-premixed flame. Appl. Phys. B **68**, 757–760 (1999)

12. J. Hult, G. Josefsson, M. Aldén, C.F. Kaminski, Flame front tracking and simultaneous flow field visualisation in turbulent combustion, in *Proceedings of the 10th International Symposium on Applications of Laser Techniques to Fluid Mechanics*, Instituto Superior Técnico, Lisbon, 2000, Paper No. 26-2

13. C.F. Kaminski, J. Hult, M. Aldén, S. Lindenmaier, A. Dreizler, U. Maas, M. Baum, Spark ignition of turbulent methane/air mixtures revealed by time-resolved planar laser-induced fluorescence and direct numerical simulations. P. Combust. Inst. **28**, 399–405 (2000)

14. C. Heeger, B. Böhm, S.F. Ahmed, R. Gordon, I. Boxx, W. Meier, A. Dreizler, E. Mastorakos, Statistics of relative and absolute velocities of turbulent non-premixed edge flames following spark ignition. P. Combust. Inst. **32**, 2957–2964 (2009)

15. B. Peterson, V. Sick, Simultaneous flow field and fuel concentration imaging at 4.8 kHz in an operating engine. Appl. Phys. B **97**, 887–895 (2009)

16. N. Soulopoulos, J. Kerl, T. Sponfelder, F. Beyrau, Y. Hardalupas, A.M.K.P. Taylor, J.C. Vassilicos, Turbulent premixed flames on fractal-grid-generated turbulence. Fluid Dyn. Res. **45**, 061404 (2013)

17. I. Boxx, M. Stöhr, C. Carter, W. Meier, Sustained multi-kHz flame front and 3-component velocity-field measurements for the study of turbulent flames. Appl. Phys. B **95**, 23–29 (2009)

18. M. Juddoo, A.R. Masri, High-speed OH-PLIF imaging of extinction and re-ignition in non-premixed flames with various levels of oxidation. Combust. Flame **158**, 902–914 (2011)

19. R. Wellander, M. Richter, M. Aldén, Time-resolved (kHz) 3D imaging of OH PLIF in a flame. Exp. Fluids **55**, 1–12 (2014)

20. R. Wellander, M. Richter, M. Aldén, Time resolved, 3D imaging (4D) of two phase ow at a repetition rate of 1 kHz. Opt. Express **19**, 21508–21514 (2011)

21. W.R. Lempert, P.F. Wu, B. Zhang, R.B. Miles, J.L. Lowrance, V.J. Mastocola, W.F. Kosonocky, *Pulse Burst Laser System for High Speed Flow Diagnostics*, AIAA-96-0179 (1996)

22. W.R. Lempert, P.F. Wu, B. Zhang, and R.B. Miles, *Filtered Rayleigh Scattering Measurements Using a MHz Rate Pulse-Burst Laser System*, AIAA-97-0500 (1997)

23. B. Zhou, C. Brackmann, Z. Li, M. Aldén, X.-S. Bai, Simultaneous multi-species and temperature visualization of premixed flames in the distributed reaction zone regime. P. Combust. Inst. **35**, 1409–1416 (2014)

24. E. Kristensson, Z. Li, E. Berrocal, M. Richter, M. Aldén, *Instantaneous 3D imaging of flame species by means of coded laser illumination* (P. Combust, Inst, 2016). in press